

Geophysical Research Letters

RESEARCH LETTER

10.1029/2021GL094594

Key Points:

- Muon flux changes during TGE reveal the charge structure of the thundercloud
- The muon stopping effect is confirmed by simulation
- Muon charge ratio is the most sensitive parameter for the identification of the inverse dipole

Correspondence to:

A. Chilingarian,
chili@aragats.am

Citation:

Chilingarian, A., Hovsepyan, G., & Zazyan, M. (2021). Muon tomography of charged structures in the atmospheric electric field. *Geophysical Research Letters*, 48, e2021GL094594. <https://doi.org/10.1029/2021GL094594>

Received 3 JUN 2021

Accepted 13 AUG 2021

Muon Tomography of Charged Structures in the Atmospheric Electric Field

A. Chilingarian^{1,2} , G. Hovsepyan¹, and M. Zazyan¹

¹A. Alikhanyan National Lab (Yerevan Physics Institute), Yerevan, Armenia, ²National Research Nuclear University MEPhI, Moscow, Russia

Abstract We compare simulations of muon traversal in the atmosphere and observation of the muon flux made on the Earth's surface to reveal the relation of the muon flux changes to the charge structure of the lower part of the thundercloud. The results show that the changes in the muon flux during large thunderstorm ground enhancements (TGEs) reveal the charge configurations of the cloud, namely a large negative electric field in the lower part of the cloud and an inverted dipole. Cosmic ray muons do not originate particle avalanches in the thunderclouds, like electrons. However, in the thundercloud, the positive and negative muons are decelerated or accelerated according to the sign of the intracloud electric field. Due to the charge asymmetry of the muon flux (excess of positive muons over negative), the total number of muons and muon charge ratio also changes.

Plain Language Summary The charged structures of the thundercloud, which initiated electron acceleration and lightning flashes, are still not well known. In the submitted letter, we examine the cosmic ray muon flux disturbances correlated with the charged structures of the thundercloud. At Aragats research station, we 24/7 monitor almost all species of secondary cosmic rays, near-surface electric field, and register atmospheric discharges. The disturbances of the muon flux were used for the tomography of the atmospheric electric field evolving during thunderstorms. Our goal is to relate the disturbances of the atmospheric electric field to changing fluxes of the elementary particles, which propagate through the cloud. Our findings will help to reveal the unusual charge structures in the cloud by monitoring of the muon flux with the simple and reliable particle detectors, also described in the letter.

1. Introduction

The electric field in the lower part of the thundercloud plays a key role in developing the relativistic runaway electron avalanches (RREAs), which reaching and are registered on the Earth's surface as thunderstorm ground enhancements (TGEs). Different species of cosmic rays, which include electrons, positrons, muons, gamma rays, and neutrons, were directly or nondirectly modulated by the intracloud electric field and comprise multisensory messengers bringing information on the electric fields emerging in the thundercloud. Recently, we used the measurements of the near-surface (NS) electric field, the graupel fall, and the energy spectra of electrons and gamma rays to get insight into the charge structure of the lower dipole and to estimate the maximum electric field in the thundercloud (Chilingarian et al., 2021a, 2021c). We considered the depletion of the muon flux as an evidence of a large negative electric field in the lower part of the thundercloud, which accelerates electrons downward and initiates electron-gamma ray avalanches. As a basic configuration of the thundercloud charge structure, we accept a classical tripole (Kuettner, 1950). For a normal three-layered tripole, the lower positively charged region (LPCR) has a smaller size and smaller charge than the upper main layers, negatively (MN) and positively charged (MP). However, alternative charge configurations were reported (see Rust et al., 2005, and references therein) inverted polarity dipole (Nag & Rakov, 2012), i.e., charge regions having a positive charge above the negative one in the vertical distribution of charge. Such structures are rare and rather difficult to identify. In the famous work (Nag & Rakov, 2009), authors conclude that the occurrence of pronounced preliminary breakdown (PB) pulse train proves the existence of an unusually large LPCR.

We outline two main scenarios (Chilingarian et al., 2020) supporting the origination of the large fluxes of electrons and gamma rays measured by the particle detectors and spectrometers located on the mountain altitudes. The first one is related to the large main negative charge above the detectors site at an altitude of

2–3 km, and the second—with emerging lower positively charged region above particle detectors. In the second scenario, both emerged electric fields have the same direction inside the cloud and can boost overall potential drop and lead to more intense TGE flux and larger maximum energy of the TGE electrons. As the electrons are very fast attenuated in the atmosphere after leaving the accelerating field, by comparison of the maximum energies of gamma ray and electron spectra we can estimate the height where the electric field declines (see Figure 9 in Chilingarian et al. (2021b)). The electric field induced by the dipole formed by the main negative layer and its mirror in the Earth (MN-MIRR) can extend down very low (25–100 m) above the Earth's surface. Additional information about charge structure we can obtain from the graupel fall, carrying the positive charge of the LPCR. A special pattern on the glass of the panoramic camera, that monitors skies above Aragats were identified to be originated by the conical graupel fall (see Figures 11 and 12 of Chilingarian et al. (2021a)). Thus, we can show that a few minutes of positive near-surface (NS) electric field coincides with minutes of the graupel fall. Usually, in the same minutes, we observe the maximum of the TGE particle flux.

The cosmic ray muons do not originate showers as electrons. However, positive and negative muons also are accelerated or decelerated according to the intracloud electric field direction. By the simulations with the CORSIKA (COsmic Ray SIMulations for KAscade, Heck et al., 1998) code we investigate how the electric field in the lower dipole modulates muon fluxes and how the observed modulation effects can be used as a probe of the intracloud electric field.

2. SEVAN Detector's Efficiency to Measure Cosmic Ray Secondary Particles

Particle detectors located on Aragats mountain are monitoring secondary cosmic ray flux, including electrons and positrons, gamma rays, muons, and neutrons. The data stream from the SEVAN detector (Chilingarian et al., 2018) which is in operation since 2008 comprises 1-min count rates from three stacked scintillators interlayered by lead filters, see Figure 1. All possible combinations of signals from three scintillators are stored as well, for instance, the “100” combination—signal was only in the upper layer; “111”—signal comes from all three layers.

The efficiency of particle selection by SEVAN coincidences was estimated by GEANT4 simulations, see Table 1. The TGE electrons and gamma rays with energies above 7 MeV are selected by “100” coincidence, the efficiency of muon selection by this coincidence is also very high; however, TGE comprises electron and gamma ray flux, vertical muon flux can be changed by only a few percent during TGE, thus, time series of the “100” coincidence apparently show the enhancement of electron and gamma ray flux and are used for estimation of the TGE significance and time of the TGE occurrence. In turn, the high-energy muons (>200 MeV) are selected by the “111” coincidence with purity above 90%, because of the lead filter, in which lower energy TGE particles are absorbed (the maximum energy of TGE electrons and gamma rays do not exceed 60 MeV). Thus, by different coincidences of the SEVAN detector, we can measure simultaneously “purified” fluxes of the cosmic ray (CR) muons and TGE particles.

3. Four Types of NS Electric Field Disturbances

NS electric field is a superposition of the fields induced by charged regions in the cloud and is highly influenced by a charge nearby to the Earth's surface. In Figure 2, we show disturbances of the NS electric field along with the count rates of TGE particles registered by a 60-cm thick and 4 m² area plastic scintillator (Figures 2a1–2d1), and below the count rates of the TGE particles registered by the SEVAN detector coincidences: “100”—electrons and gamma rays and “111”—high-energy muons (Figures 2a2–2d2). Throughout this letter, we use the atmospheric electricity sign convention, according to which the downward directed electric field or field change vector is positive.

In Figures 2a2–2c2 and Table 2, we can see that due to the muon stopping effect (see Chilingarian et al., 2021a, and references therein), simultaneously with TGE particles flux enhancement (>10%) we observe depletion of the muon flux (1.7–8%). The significance of the TGE flux enhancement measured in the number of standard deviations from the mean value at fair weather is very large, 12–17 σ for the 1-min time

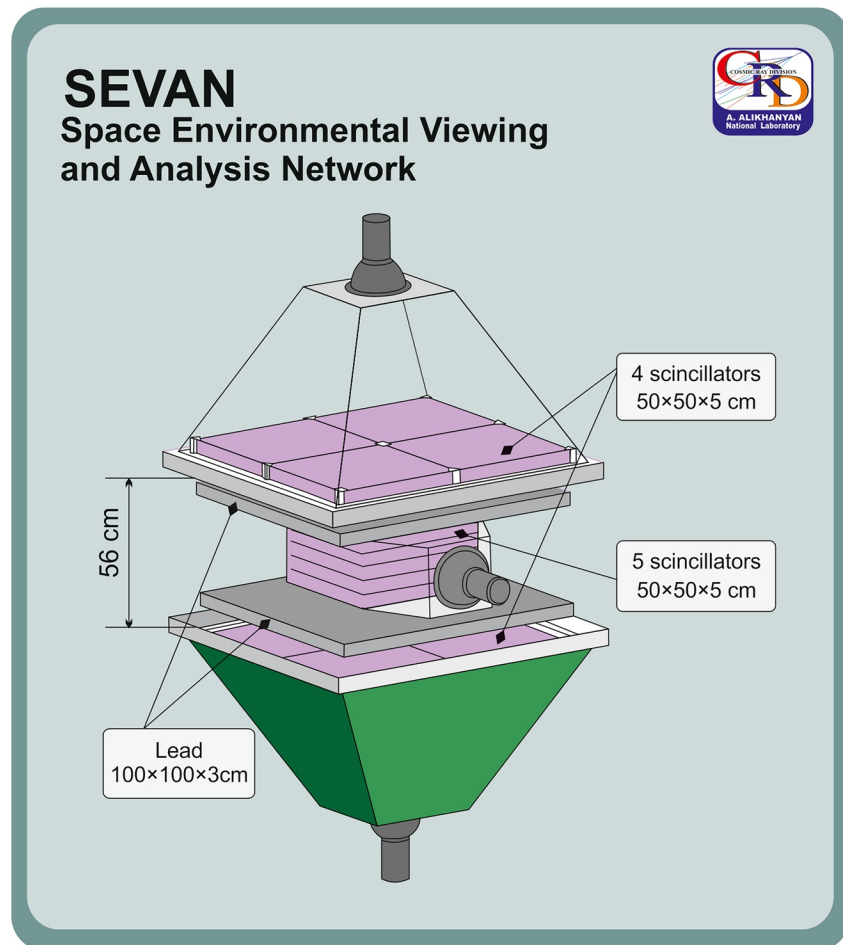


Figure 1. The design of the SEVAN unit located on Mt. Aragats.

series. Also, as it is seen from frames (a2), (b2), (c2), the depletion of muon flux also is apparent during the whole time of TGE, although the significance is much lower.

Fluctuations of the 1-min count rate of the “111” coincidences are larger than fluctuations of “100” coincidences. Also, we select for the analysis, the raw TGE events of 2020, the flux enhancement of the largest TGE events we analyze in Chilingarian et al. (2021a, 2021c) was much larger and muon depletion—much deeper.

The muon flux decline can occur a few minutes after (or before) the TGE maximum. TGE particles arrive at the detector from the near-vertical direction, in turn, a deficit of muon flux originates mostly from the inclined trajectories because the maximum of the muon flux is at a zenith angle of $\approx 21^\circ$ (see also Figures 6 and 8 of Chilingarian et al. (2021a)). Thus, slightly different parts of the electrified atmosphere are responsible for the TGE flux enhancement and for the muon depletion, and the minutes of maximum effect can be shifted from each other. Only in frame 2d2, we see enhancement of the muon flux a minute after the maximum of the TGE flux. Various patterns of the observed NS electric field disturbances that support the TGE initiation, shown in Figure 2 can be described as follows:

1. The particle flux started to rise when the field reversal from the positive to the negative values occurred and reaches the maximum when the field dropped in the deep minimum reaching ≈ -25 kV/cm (Figure 2a1). After a main phase of the TGE, on the second field reversal from the negative to positive, the decay of TGE stopped and during the positive NS electric field, TGE continuous with smaller amplitude. RREAs of this type are originated from the electric field of the dipole formed by the MN layer in the middle of the cloud and its mirror image in the Earth

Table 1
SEVAN Detector Efficiencies for Detecting Different Species of Secondary Cosmic Rays Conditioned on Registered Coincidences of SEVAN Detector Channels

| Energy (MeV) | Neutron (%) | Mu+ (%) | Mu- (%) | Electron (%) | Positron (%) | Gamma (%) |
|---|-------------|---------|---------|--------------|--------------|-----------|
| SEVAN detector coincidence “100” (TGE electrons and gamma rays) | | | | | | |
| 7 | 34.01 | 42.10 | 13.96 | 1.42 | 3.38 | 1.93 |
| 10 | 52.70 | 46.18 | 15.30 | 51.18 | 51.82 | 5.67 |
| 15 | 48.91 | 91.52 | 90.11 | 75.59 | 72.07 | 7.35 |
| 20 | 38.81 | 95.02 | 93.93 | 77.12 | 72.80 | 7.97 |
| 30 | 29.07 | 96.86 | 97.01 | 81.61 | 76.88 | 8.49 |
| 40 | 28.33 | 98.78 | 98.94 | 88.54 | 84.18 | 8.63 |
| SEVAN detector coincidence “111” (high-energy muons) | | | | | | |
| 100 | 0.31 | 0.13 | 0.09 | 0.27 | 0.28 | 0.01 |
| 200 | 0.92 | 45.58 | 50.33 | 3.12 | 3.37 | 0.22 |
| 300 | 1.84 | 86.36 | 86.34 | 8.69 | 8.86 | 0.71 |
| 350 | 2.26 | 84.19 | 84.23 | 11.90 | 11.89 | 1.08 |
| 380 | 2.82 | 83.03 | 82.99 | 14.02 | 14.00 | 1.22 |
| 400 | 3.07 | 82.04 | 82.15 | 15.33 | 15.19 | 1.39 |

2. After several lightning flashes, NS electric field was almost constant for 10 min in the positive domain of ≈ 20 kV/m (Figure 2b1). RREAs of this type are originated by the electric field of two dipoles which accelerate electrons in the cloud in the direction to the Earth’s surface: accelerating field of the MN-MIRR dipole is enhanced in the cloud by the MN-LPCR dipole. After leaving the region of the strong accelerating field the electric field originated by the LPCR-MIRR dipole will decelerate electrons and negative muons and accelerate positive muons
3. During the negative NS field an uprise occurred that significantly enhance the field values for a few minutes. The maximum amplitude of TGE coincides with a maximum of the NS field during this uprise (Figure 2c1). At the returning of the field to the negative domain TGE smoothly declines. No nearby lightning flashes were observed
4. A minute after TGE maximum we detect a maximum of high-energy muon flux (Figure 2d2). Such events are very rare; we identify only one at Aragats for the whole time of observations and two in Lomnicky Stit. The muon flux enhancement occurred after a few minutes of the positive field and a –CG lightning flash that abruptly terminates TGE (Figure 2d1)

From Figure 2, we can deduce that during time intervals of several minutes when the near-surface electric field was in positive domain with approximately constant amplitude (Figure 2b1—12:59–13:09 and Figure 2d1—11:24–11:28), the LPCR is rather low above detectors and has

a relatively large positive charge enough to “screen” the detector site from the main negatively charged region in the middle of the cloud. The horizontal extent of LPCR is also sizable that demonstrates the large depletion of the inclined muon trajectories. This effect is especially strong on the sharp mountain peaks and reaches 20–45% at Lomnicky Stit and Musala mountains (see Figures 2c and 3c in Chilingarian et al. (2021c)).

To understand the described above modulation effects posed by the strong electric fields (exceeding the critical field value to force CR electrons to runaway), we perform a cycle of simulations starting from the entrance of the galactic protons into the terrestrial atmosphere to the Earth’s surface.

4. Simulation of the CR Muons Traversal in Thunderous Atmosphere

We simulate the extensive air shower (EAS) initiated by the high-energy primary proton entering the terrestrial atmosphere. The energy spectrum of primary protons follows the power law with the spectral index of -2.7 ; the *energy range* of primary protons was $10\text{--}1,000$ GeV. High-energy interactions of cosmic rays with the Earth’s atmosphere have been simulated by means of the CORSIKA code (Heck et al., 1998) with strong interaction models QGSJETII-04 (Ostapchenko, 2011) and UrQMD (Bass et al., 1998). We used the CORSIKA 7.7400 version which takes into account the effect of the electric field on the transport of particles (Buitnik et al., 2010). Primary cosmic ray protons originate EASs high in the atmosphere, secondary electrons and muons from these EASs enter the vertical region of the uniform electric field with strengths exceeding the runaway threshold (critical energy) by a few tens of percent on 2–3 km height above the Aragats station. The parameters of the atmospheric electric field were the same as in our previous RREA modeling studies (Chilingarian et al., 2021a, 2021c). Secondary particles were followed until hadron energies diminished down to 300 MeV and muon energies—to 100 MeV. The electric field strengths at the heights of 3,400–5,400 m were chosen in the range from 1.8 to 2.2 kV/cm. Smaller fields will not generate avalanches with a significant number of electrons (no TGE will occur), and higher fields will result in a very large number of electrons, which will make enough ionization to assist lightning leaders to reach the Earth’s surface and initiate a cloud-ground flash terminating TGE. In CORSIKA, there are no options of lightning initiation, thus we restrict ourselves in the simulations to the mentioned values of electric field strength because higher fields are unphysical.

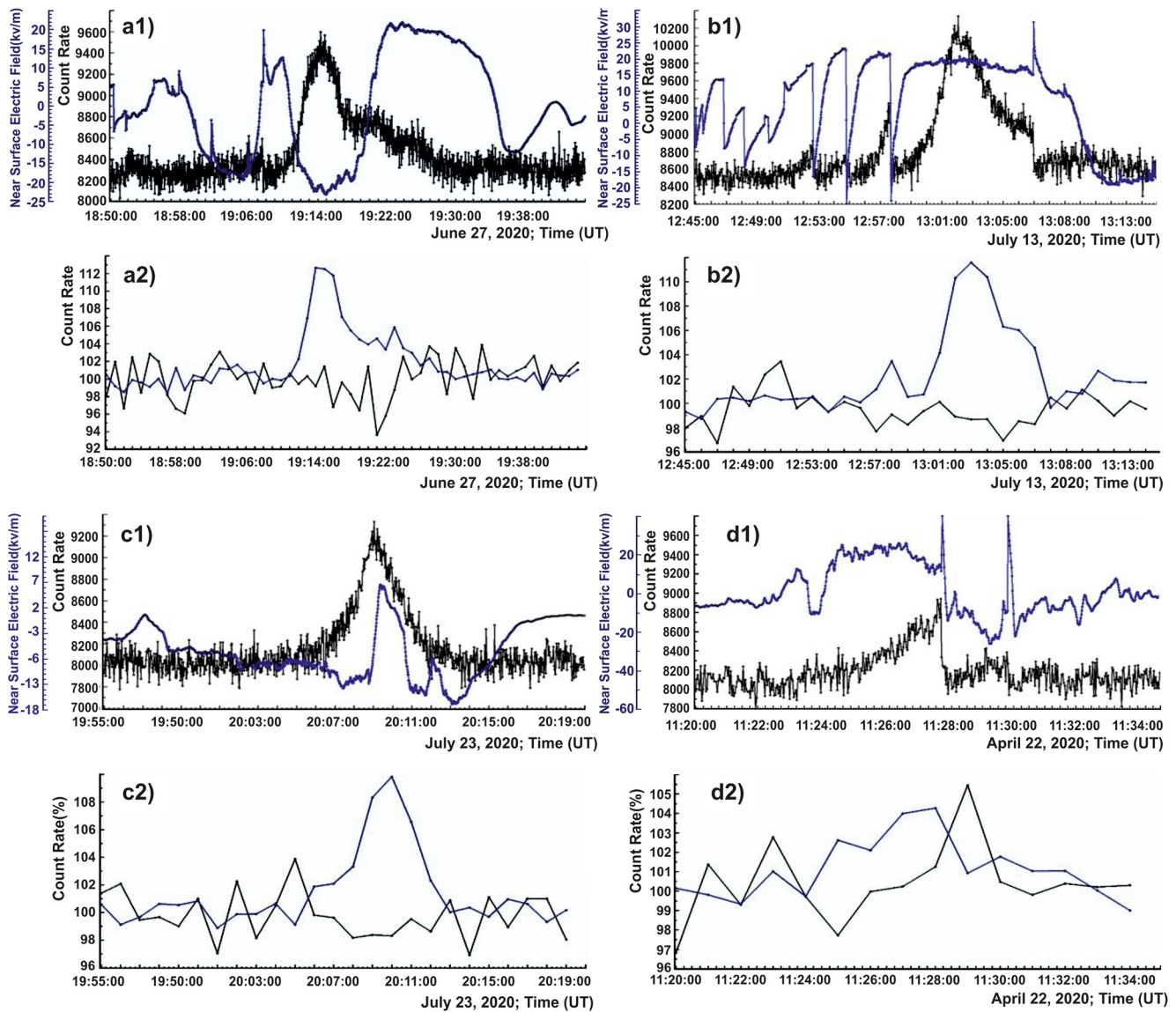


Figure 2. Four different modes of near-surface (NS) electric field disturbances and corresponding changes of the high-energy muon fluxes. In a1–d1 frames, we show the time series of the 60-cm thick and 4 m² area plastic scintillator (black) and –NS electric field disturbances measured by the EFM-100 electric mill located on the roof of the MAKET experimental hall (blue). In frames a2–d2, we show the time series of SEVAN’s “100” coincidences (blue, mostly electrons and gamma rays) and “111” (black, mostly muons). Count rates of particle detectors are shown as a percent to fair weather value measured before thunderstorm ground enhancement (TGE) started.

As we can see in Figure 3, every 300 m we calculate the number of muons per primary proton for opposite strengths of the intracloud electric field (2.1 and –2.1 kV/cm). The depth in the atmosphere equals zero meters at 5,400 m a.s.l. where we introduce the electric field, and –2,000 m at 3,400 m where the electric field ended. The remaining 200 m until particle detectors, muons propagate in the air without any electric field. From 5,400 to 3,200 m, the flux continuously decreased due to muon decay (the muon flux maximum is at ≈15-km altitude). The upward-directed field suppresses positive muon flux (blue curve in Figure 3b), confirming muon flux depletion during TGEs, see Figures 2a2–2c2. Accordingly, the oppositely directed field highly suppresses negative muon flux (green curve in Figure 3a) and, sure, for this direction of the electric field, no TGE is possible. The most sensitive to the intracloud field direction is the

Table 2
Percent of the Flux Enhancement and Number of Standard Deviations From the Mean Value Measured on Fair Weather for the TGE Particles and Muons Measured by SEVAN Detector

| Coincidence | June 27, 2020 | July 13, 2020 | July 23, 2020 | April 22, 2020 |
|-------------|---------------|---------------|---------------|----------------|
| “111” | –8%/–5σ | –2.5%/–1.6σ | –1.7%/–0.7σ | 5.7%/3.1σ |
| “100” | 14%/17σ | 12%/15σ | 10%/12σ | 4.6%/6.5σ |

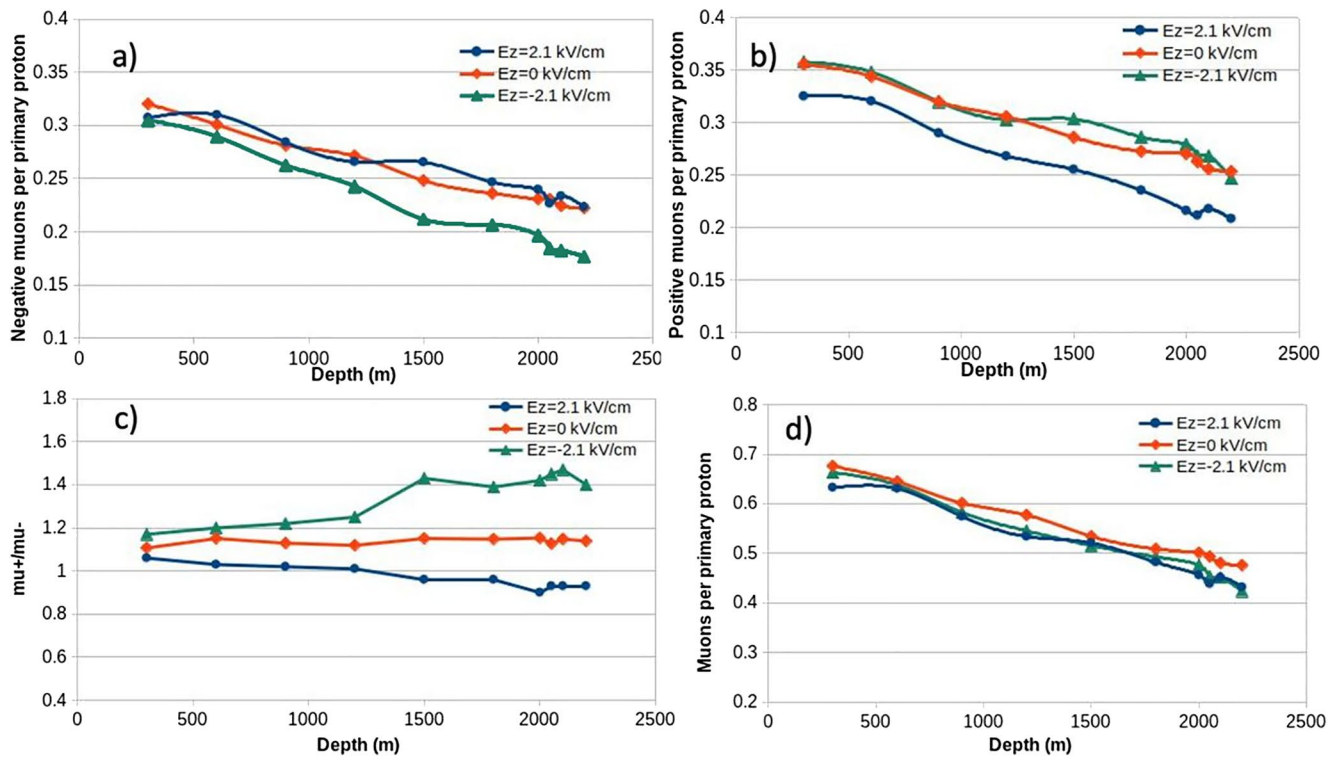


Figure 3. Development of the muon flux traversing the strong electric field region located at 3,400–5,400 m; after leaving the field region muons cross additional 200 m until reaching the Earth’s surface.

muon charge ratio parameter (the ratio of positive to negative muons), see Figure 3c. The value of the muon charge ratio at 3,200 m (depth in atmosphere 2,200 m) for two opposite fields is drastically different (1.4 and 0.9, see Figure 3c). Thus, by measuring the charge ratio and if it is significantly larger than the 0-field value (for instance 1.4, as in Figure 3c) we can deduce that there is a positive dipole (positive charge above negative) in the lower part of the cloud. The overall depletion comparing with no-field simulations for both field directions is shown in Figure 3d. The depletion of the muon flux reaches 8% for the field strength of 2.1 kV/cm. The Aragats SEVAN measurements show smaller depletion due to lower strength of the intra-cloud electric field for the raw events that initiated not very large TGEs measured in 2020.

The muon flux enhancement shown in Figure 2d2 cannot be explained by the modeling trials shown in Figure 3. To reproduce this very rare enhancement of muon flux during TGE, we perform another trial of CORSIKA simulations.

In the second trial of simulations, we examine the influence of the emerged LPCR on the muon flux intensity. Muons cross the same 2 km distance in the strong electric field from 6,200 to –4,200 m, and after leaving the accelerating electric field enter the opposite direction field region with a lower strength of 1.2 kV/cm (a field region where MN-MIRR and LPCR-MIRR electric fields are oppositely directed). Thus, positive muons that initially be decelerated in the thundercloud after traversing the LPCR will be accelerated by the oppositely directed electric field between LPCR and the Earth’s surface. However, with assumed extreme and extended field configuration, we cannot reproduce the enhancement of the muon flux during TGE, shown in Figure 2d2. As we can see in Figure 4, the muon total flux did not surpass the 0-field value. For any tested configuration of the electric field strength and extent, we cannot obtain

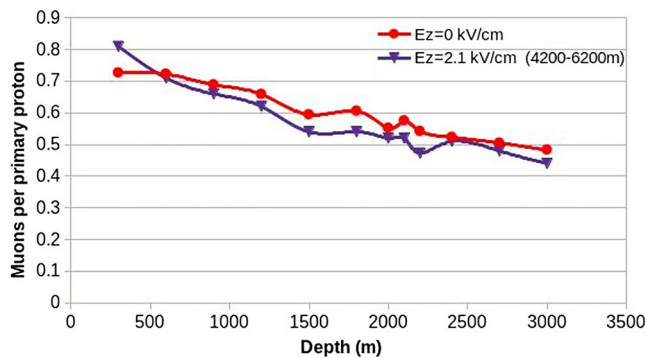


Figure 4. After muon traversal in the field of 2.1 kV/cm located at 4,200–6,200 altitudes, muons cross 1,000 m from 4,200 to 3,200 until be registered. The electric field in the 1,000 m gap was +1.2 kV/cm.

enhancement of the muon flux during TGE (simultaneously with the large enhancement of electron and gamma ray flux).

5. Conclusions

In the present letter, we consider different types of muon flux disturbances measured during thunderstorm ground enhancements, including very rare ones (Figure 2). As well, we simulate with CORSIKA code the possible modulation of the parameters of the muon flux by the intracloud electric field to reveal the structure of the intracloud electric field. CORSIKA code was started now not from the secondary electrons, but from the primary high-energy protons entering the terrestrial atmosphere. The muon flux measurements and appropriate simulations confirm the relation of the muon flux disturbances to the charged structures emerging in the lower part of the thundercloud. We confirm the muon stopping effect, used in our previous papers for the estimation of the maximum electric field in the thundercloud.

Based on SEVAN measurements and CORSIKA simulations, we can conclude that the muon charge ratio is the most sensitive parameter for determining the charge structure in the cloud (Figure 3c). By measuring the muon charge ratio, the inverted dipole structure can be easily identified. The possibility of construction of the magnetic spectrometer with maximum detectable momentum of ≈ 300 MeV is discussed now.

By changing various simulation parameters, we were unable to reproduce very rare measurements of enhancement of muon flux during TGE. In our simulations, the muon flux was not sensitive to the electric field in the gap between the cloud and the Earth's surface. Thus, even for the LPCR having an unusually large charge and vertically extend, we cannot obtain enhanced muon flux as was measured by the SEVAN detector on April 22, 2020 (see Figures 2d2 and 4).

Data Availability Statement

The data for this study are available in numerical and graphical formats by the multivariate visualization software platform ADEI (Chilingaryan et al., 2008) on the WEB page of the Cosmic Ray Division (CRD) of the Yerevan Physics Institute, <http://adei.crd.yerphi.am/adei>.

Acknowledgments

We thank the staff of the Aragats Space Environmental Center for the uninterrupted operation of experimental facilities on Aragats under severe weather conditions. The authors thank S. Soghomonyan for useful discussions and help in preparing the manuscript.

References

- Bass, S., Belkacem, M., Bleicher, M., Brandstetter, M., Bravina, L., Ernst, C., et al. (1998). Microscopic models for ultrarelativistic heavy ion collisions. *Progress in Particle and Nuclear Physics*, *41*, 255–369. [https://doi.org/10.1016/s0146-6410\(98\)00058-1](https://doi.org/10.1016/s0146-6410(98)00058-1)
- Buitink, S., Falcke, H., Huege, T., Heck, D., & Kuijpers, J. (2010). Monte Carlo simulations of air showers in atmospheric electric fields. *Astroparticle Physics*, *33*, 1–12. <https://doi.org/10.1016/j.astropartphys.2009.10.006>
- Chilingarian, A., Babayan, V., Karapetyan, T., Mailyan, B., Sargsyan, B., & Zazyan, M. (2018). The SEVAN Worldwide network of particle detectors: 10 years of operation. *Advances in Space Research*, *61*, 2680–2696. <https://doi.org/10.1016/j.asr.2018.02.030>
- Chilingarian, A., Hovsepian, G., Karapetyan, G., & Zazyan, M. (2021a). Stopping muon effect and estimation of intracloud electric field. *Astroparticle Physics*, *124*, 102505. <https://doi.org/10.1016/j.astropartphys.2020.102505>
- Chilingarian, A., Hovsepian, G., Karapetyan, T., Karapetyan, G., Kozliner, L., Mkrtchyan, H., et al. (2020). Structure of thunderstorm ground enhancements. *Physical Review D*, *101*, 122004. <https://doi.org/10.1103/physrevd.101.122004>
- Chilingarian, A., Hovsepian, G., Svechnikova, E., & Zazyan, M. (2021b). Electrical structure of the thundercloud and operation of the electron accelerator inside it. *Astroparticle Physics*, *132*, 102615. <https://doi.org/10.1016/j.astropartphys.2021.102615>
- Chilingarian, A., Karapetyan, T., Zazyan, M., Hovsepian, G., Sargsyan, B., Nikolova, N., et al. (2021c). Maximum strength of the atmospheric electric field. *Physical Review D*, *103*, 043021. <https://doi.org/10.1103/physrevd.103.043021>
- Chilingaryan, S., Chilingarian, A., Danielyan, V., & Eppler, W. (2008). The Aragats data acquisition system for highly distributed particle detecting networks. *Journal of Physics: Conference Series*, *119*, 082001. <https://doi.org/10.1088/1742-6596/119/8/082001>
- Heck, D., Knapp, J., Capdevielle, J. N., Schatz, G., & Thouw, T. (1998). *Forschungszentrum, Karlsruhe* (Report No. FZKA 6019). Retrieved from <https://www.ikp.kit.edu/corsika/70.php>
- Kuettner, J. (1950). The electrical and meteorological conditions inside thunderclouds. *Journal of Meteorology*, *7*, 322–332. [https://doi.org/10.1175/1520-0469\(1950\)007<0322:teamci>2.0.co;2](https://doi.org/10.1175/1520-0469(1950)007<0322:teamci>2.0.co;2)
- Nag, A., & Rakov, V. A. (2009). Some inferences on the role of lower positive charge region in facilitating different types of lightning. *Geophysical Research Letters*, *36*, L05815. <https://doi.org/10.1029/2008GL036783>
- Nag, A., & Rakov, V. A. (2012). Positive lightning: An overview, new observations, and inferences. *Journal of Geophysical Research*, *117*, D08109. <https://doi.org/10.1029/2012JD017545>
- Ostapchenko, S. (2011). Monte Carlo treatment of hadronic interactions in enhanced Pomeron scheme: I. QGSJET-II model. *Physical Review D*, *83*, 014018. <https://doi.org/10.1103/physrevd.83.014018>
- Rust, D., Donald, T., MacGorman, R., Weiss, S. A., Krehbiel, P. R., Thomas, R. J., et al. (2005). Inverted-polarity electrical structures in thunderstorms in the Severe Thunderstorm Electrification and Precipitation Study (STEPS). *Atmospheric Research*, *76*, 247–271. <https://doi.org/10.1016/j.atmosres.2004.11.029>